Petroleum Science 22 (2025) 4412–4427

Contents lists available at ScienceDirect

Petroleum Science

journal homepage: www.keaipublishing.com/en/journals/petroleum-science

Original Paper

Control of fault transport ability on hydrocarbon migration and accumulation in the No. 4 structural zone of Nanpu Sag, Bohai Bay Basin, China

Xiao-Fei Fu [a,b], Ming-Xing Fan [a,*], Hai-Xue Wang [a], Ru Jia [a], Xian-Qiang Song [a], Ye-Jun Jin [a]

[a] CNPC Fault Controlling Reservoirs Laboratory, Northeast Petroleum University, Daqing, 163318, Heilongjiang, China
[b] State Key Laboratory of Continental Shale Oil, Northeast Petroleum University, Daqing, 163318, Heilongjiang, China

ARTICLE INFO

Article history:
Received 14 May 2024
Received in revised form
30 June 2025
Accepted 14 August 2025
Available online 21 August 2025

Edited by Jie Hao and Xi Zhang

Keywords:
Nanpu Sag
Fault transport ability
Hydrocarbon migration and accumulation
Reservoir formation
Quantitative evaluation

ABSTRACT

The ability of faults to transport oil and gas is affected by multiple geological factors, and the effects of various factors on oil and gas migration and accumulation are complex. In this study, based on the drilling and three-dimensional seismic data in the No. 4 structural zone of the Nanpu Sag and by considering the effects of fault throw, caprock thickness, shale content, fluid pressure, stress normal to the fault plane, and brittleness, we employed fault transport index (FTI) to quantitatively characterize the vertical transport ability of regional faults. Through statistical analysis, fault transport probability (N_p) was used to characterize the relationship between FTI and the vertical hydrocarbon content in the formations. The results show that the faults with FTI less than 0.75 cannot transport oil and gas, while those with FTI greater than 2.5 are able to transport oil and gas. Specifically, when FTI is between 0.75 and 2.5, there is a functional relationship between the probability of faults transporting hydrocarbons and FTI. The current oil and water distribution and paleo oil reservoir test results indicate that there are oil layers or paleo oil reservoirs in horizons with large N_p. Therefore, FTI can be used as an effective coefficient to indicate the vertical migration paths and accumulation spots of hydrocarbons moving along faults, providing an essential reference for further oil and gas exploration and development.

1. Introduction

The role faults play in oil and gas migration and accumulation has always been a hot topic in almost all petroliferous basins (Knipe, 1997; Fu et al., 2021, Jin et al., 2023). Numerous studies have demonstrated that faults act as channels for fluid migration or barriers hindering fluid migration (Hooper, 1991; Lv et al., 2007; Ryan et al., 2017). When a fault functions as a channel, they can not only connect with source rocks and reservoir rocks, forming preferential hydrocarbon migration channels, but can also destroy early-formed reservoirs and adjust the oil and gas inside (Gudmundsson, 2001; Song et al., 2022). The latter process may result in oil and gas moving toward shallower formations along faults, subsequently forming reservoirs or leaking. By contrast, when a fault acts as a barrier, the fault can prevent oil and gas from migrating or escaping to shallow formations along the fault (Sibson et al., 1975; Haney et al., 2005; Lv et al., 2007). In addition, investigations have shown that fault activity is periodic, characterized by intermittent opening and closing activities. Faults are often open during active periods and can serve as pathways for oil and gas migration, while they are basically closed during stable periods, preventing oil and gas from further movement (Anders and Schlische, 1994; Xu et al., 2019a; Fan et al. al, 2023). With the periodic activity of faults, pressure change in overburden rocks, and the influence of diagenesis and cementation during fluid flow, the permeability of the fault zone is in a dynamic evolution process. During different fault evolution stages, the permeability of fault nucleus and rupture zone varies significantly. Thus, faults can act as channels or blocking barriers at different stages (Bruhn et al., 1990; Caine et al., 1996; Berg and Skar, 2005; Jiang et al., 2023, 2024).

Due to the essential role that faults play in hydrocarbon migration and accumulation, numerous researchers have investigated the hydrocarbon transport ability of faults from different

* Corresponding author.
E-mail address: fanmingxing1997@163.com (M.-X. Fan).
Peer review under the responsibility of China University of Petroleum (Beijing).

https://doi.org/10.1016/j.petsci.2025.08.024

aspects (Jiang et al., 2022; Smeraglia et al., 2022; Allgaier et al., 2023; Evans et al., 2024). The active period of faults and fault morphology are two common focuses in the analysis of faults' transport ability. It was suggested that faults formed during hydrocarbon accumulation period and reactivated faults in the source area can serve as excellent channels transporting oil and gas (Im et al., 2018; Xu et al., 2019b; Smeraglia et al., 2022), and the change in fault curvature can alter stress distribution, thereby controlling oil and gas migration (Foschi and Van, 2022; Allgaier et al., 2023). By analyzing the scale and occurrence of regional faults and the effective thickness distribution, Wang et al. (2021) proposed an oil and gas migration mode controlled by both faults and the reservoir. Considering the influence of regional structure deformation on hydrocarbon migration, Lv et al. (2022) employed released and involved volumes to characterize faults' migration ability. Despite the fruitful results obtained, many qualitative hydrocarbon migration models, as well as fault-controlled hydrocarbon accumulation mechanisms proposed based on a single geological factor can no longer meet the increasingly accurate exploration requirements. Thus, quantitative analyses with the consideration of multiple geological factors are urgently needed.

After years of oil and gas exploration, seismic and drilling data collected in the No. 4 structural zone of Nanpu Sag have become completed, irrespective of the coverage or volume, and a number of significant investigations in this region have been conducted (e.g. Tong et al., 2013; Lv et al., 2015; Liu et al., 2022). Some studies suggested that the hydrocarbon distribution in the No. 4 structural zone is influenced by caprocks, and the ability of regional faults to transport oil and gas is strongly associated with fault activity rate and fault concentration (Tong et al., 2013; Lv et al., 2015). However, most relevant studies only focused on the migration ability of fault segment in the caprock layer, which limited the in-depth exploration and development in the No. 4 structural zone. In this study, based on an unprecedented number of seismic, paleo-reservoir, and drilling data, we comprehensively analyzed the influence of various geological factors on oil and gas migration, and probed the hydrocarbon transport ability of regional faults throughout multiple layers. Compared to previous research, this study conducts reliable quantitative predictions of long-fault hydrocarbon migration pathways by referring to a series of significant geological parameters (e.g. brittleness index, shale smear factor, pore-fluid pressure, etc.). This innovative method offers an essential guidance on further oil and gas exploration in the Nanpu Sag.

2. Geological setting

The Nanpu Sag is a small oil-generating sag developed in the Mesozoic and Cenozoic in the northeastern Huanghua Depression in the Bohai Bay Basin. The sag covers an area of about 1932 km^2, exhibiting a dustpan-shaped fault-depression structure with faulting in the north and onlap in the south (Fig. 1). The entire sag is composed of 7 secondary structural zones (i.e. Gaoliu structural zone, Laoyemiao structural zone, and Nanpu No. 1–5 structural zone) and 4 sub-sags (i.e. the Shichang, Linque, Caofeidian and Liunan sub-sags) (Pang et al., 2019). During the Cenozoic, the Nanpu Sag has experienced the Paleogene extensional fault depression stage and the Neogene subsidence stage, and the regional faults are highly developed (Tong et al., 2013; Lv et al., 2015). The strata inside the sag include the pre-Tertiary basement and Paleogene and Neogene formations. Compared with other sags in the Bohai Bay Basin, the Paleogene strata of the Nanpu Sag lack the Kongdian Formation and the fourth member of Shahejie Formation (Fig. 2). Specifically, the Paleogene strata include the Shahejie Formation (Es) and Dongying Formation (Ed), and the Neogene strata include the Guantao Formation (Ng), Minghuazhen (Nm) and Quaternary strata (Wang et al., 2008; Jiang et al., 2018). Totally three sets of source rocks, namely the third member of Shahejie Formation (Es_3), the first member of Shahejie Formation (Es_1) and the third member of Dongying Formation (Ed_3), are developed in the Nanpu Sag. The comparison results of biomarkers and monomeric hydrocarbon carbon isotopes indicate that the shallow oil and gas in the No. 4 structural zone are genetically associated with the source rocks of the first member of Shahejie Formation and the third member of Dongying Formation, which are thus considered the main source rocks (Li et al., 2011; Gao et al., 2021). Notably, oil and gas are vertically active in the No. 4 structural zone, with hydrocarbon show observed from the third member of Shahejie Formation to the Minghuazhen Formation. Fluid inclusion data show that the hydrocarbon charging period of the No. 4 structural zone is late, mainly from the late Minghuazhen period to Quaternary (3–0.5 Ma) (Zhu et al., 2011; Wan et al., 2013). Previous studies have shown that there are three periods of strong fault activity in Nanpu Depression, namely, the extensional deformation period in the deposition period of the third member of Shahejie Formation, the strike-slip extensional deformation period in the deposition period of the first member of Dongying Formation and the tension-torsion deformation period in the deposition period of Minghuazhen Formation–Quaternary System (Lv et al., 2015). Liu et al. (2024) suggested that the fault activity rate during the sedimentary period (accumulation period) of Minghuazhen Formation in Nanpu Sag is 1.6–31.3 m/Ma, with an average of 11.2 m/Ma, while the fault activity rate of the No. 4 structural zone is 3.1–18.8 m/Ma, with an average of 11 m/Ma. Active faults play an important role in vertical migration of oil and gas during accumulation period, and oil and gas are mostly distributed near these faults (Zhang et al., 2011; Liu et al., 2022). The main object of this paper is the faults (F1–16) that were active during the accumulation period.

3. Methods

3.1. Factors affecting along-fault migration of hydrocarbons and the corresponding quantitative characterization method

3.1.1. Degree of shale smear

Shale smear refers to all the processes that transform shale in surrounding rocks into shaly materials in fault zones. Due to the competence difference in sand-shale formations, shale is often involved in fault zones through grinding, shearing, and injection, etc. (Vrolijk et al., 2016). Factors that control shale smear include the thickness of the shale layer, fault throw, and the number of shale layers (Berg and Avery, 1995; Yielding et al., 2002). Experimental studies have confirmed that the degree of shale smear will change with different shale content under the same conditions. The greater the shale content, the wider the range of shale smear and the better the continuity (Giger et al., 2013). Based on the generalized shale smear factor simplified by Yielding et al. (1997), this study proposed a smear factor (SF) that considers the influence of shale content on shale smear. The factor was used to characterize the proportion of shale or clay that may be carried by various mechanisms in the fault zone (Eq. (1)):

$$\mathrm{SF} = \sum_{i=1}^{n}\left(\frac{V_{\mathrm{sh}}\Delta Z_i}{D}\cdot 100\%\right) \tag{1}$$

where SF refers to smear factor (dimensionless); V_{sh} denotes the shale content, %; ΔZ_i is the shale thickness of the ith layer, m; and D is the fault throw, m. The shale content and thickness can be acquired from the drilling data, while the fault throw can be obtained from the seismic interpretation data.

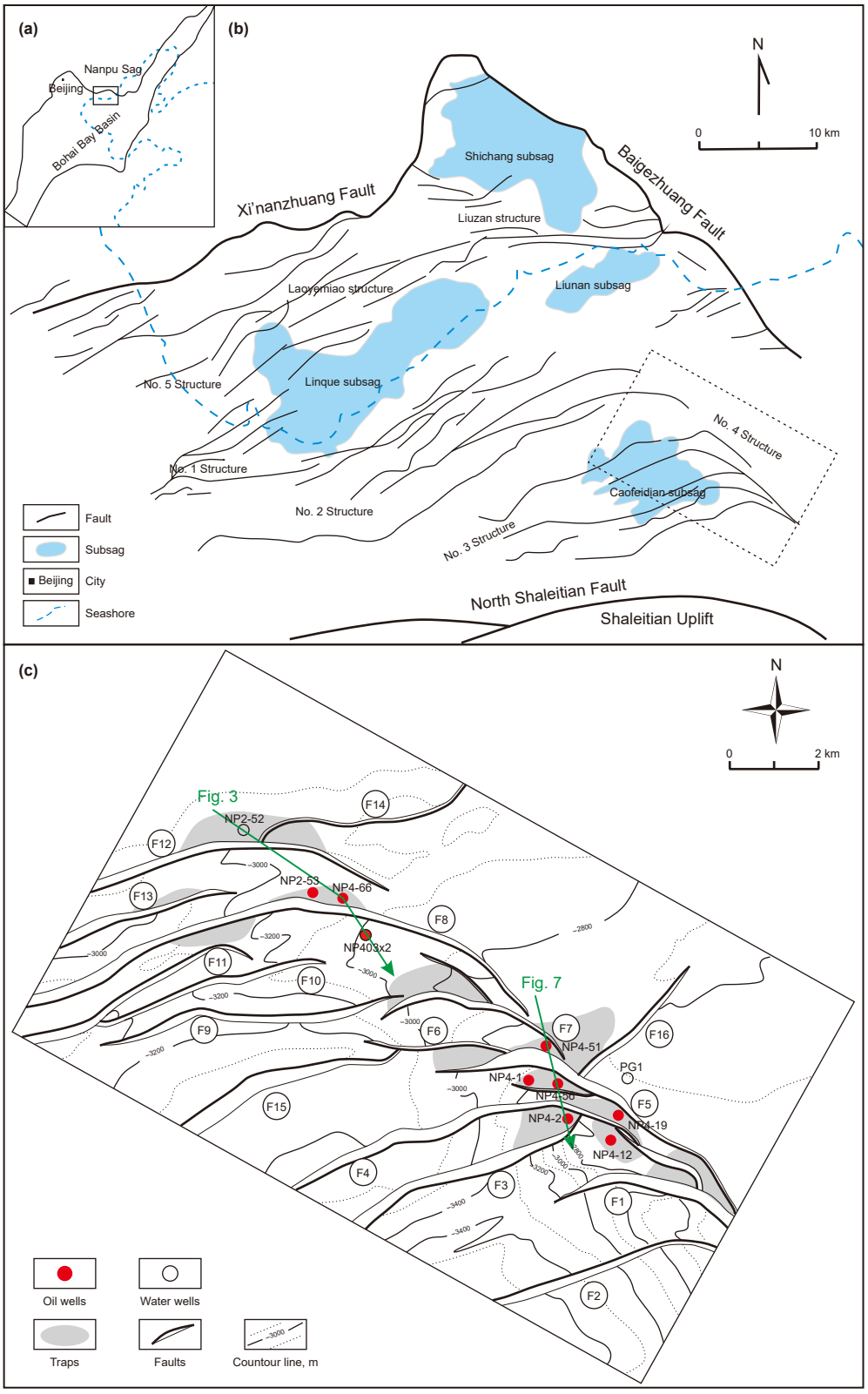

Fig. 1. **(a)** Location of the Nanpu Sag in Bohai Bay Basin. **(b)** Structural units in the Nanpu Sag. **(c)** Bottom surface structural map of the second member of Dongying Formation of the No. 4 Structure, the green arrow line is the track of Figs. 3 and 7.

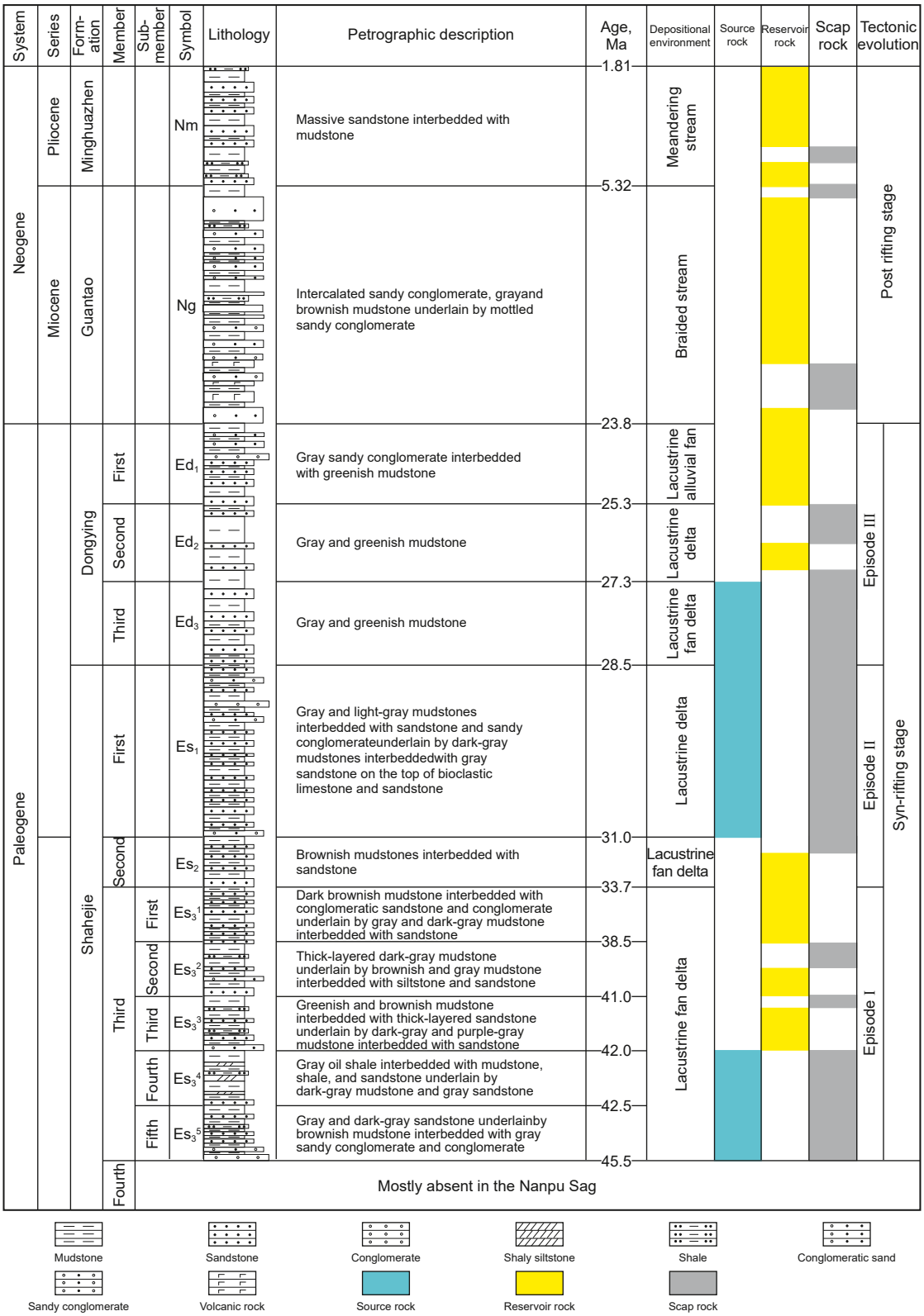

Fig. 2. Feature map of stratigraphic and tectonic evolution as well as the source-reservoir-seal combination of Nanpu Sag (modified according to Jiang et al., 2018).

3.1.2. The normal stress acting on the fault plane

The normal stress acting on the fault plane (also called normal stress in this study) is closely related to the vertical sealing ability of faults (Jones and Hillis, 2003; Wang and Dai, 2012) and directly affects the degree of tightness of the fault plane. If the fault plane is tightly closed, the vertical sealing of the fault is good, and it is difficult for oil and gas to move vertically; otherwise, the fault can act as a channel for oil and gas migration (Lv et al., 1996).

Additionally, large normal stress often leads to plastic deformation of rocks in the fault zone, thus reducing the porosity and permeability of the fault zone and even leading to the closure of cracks inside (Harding and Tuminas, 1989). Annular shear experiments also indicated that with the increase of normal stress, the possibility of forming a continuous shale smear increase, the continuity of the shale smear and the shale-covered area increase, and the possibility of vertical fault sealing ability increases (Sperrevik et al., 2000; Clausen and Gabrielsen, 2002).

The stress normal to the fault plane can be calculated based on the location and direction of the fault, as well as the information of the underground stress field (Jaeger et al., 2009). The hydrocarbon charging period in the No. 4 structural zone is late (Zhu et al., 2011; Wan et al., 2013), and thus this study used the current stress magnitude and direction to approximately represent those in the reservoir formation period. The vertical stress is mainly caused by the self-weight of the overburden rock and can be obtained by integrating the density log data (Eq. (2)):

$$\sigma_v = \rho_w g h_w + \int_0^h \rho(h) g \mathrm{d}h \tag{2}$$

The horizontal principal stress was calculated using the Huang's model considering that the horizontal in-situ stress in underground rock formations is mainly generated by the overburden rock pressure and the horizontal tectonic stress. The horizontal tectonic stress is directly proportional to the pressure caused by the overburden rock (Huang, 1984) (Eqs. (3) and (4)). Then, the relationship between the principal stress and the normal angle of the fault plane and the occurrence of the fault was established. The normal stress of the fault can be calculated through the effective normal stress calculation formula (Eq. (5)):

$$\sigma_H = \left(\frac{\mu}{1-\mu} + \beta_1\right)(\sigma_v - \alpha P_p) + \alpha P_p \tag{3}$$

$$\sigma_h = \left(\frac{\mu}{1-\mu} + \beta_2\right)(\sigma_v - \alpha P_p) + \alpha P_p \tag{4}$$

$$\sigma_N = (\sin\theta_1 \sin\theta_2)2\sigma_H + (\cos\theta_1 \sin\theta_2)2\sigma_h + \cos\theta_2 \sigma_v \tag{5}$$

where σ_H, σ_h and σ_v represent the horizontal maximum, minimum in-situ stress and vertical in-situ stress, MPa; σ_N is the stress normal to the fault plane, MPa; respectively, θ_1 is the Angle between the section strike and the maximum horizontal principal stress, °; θ_2 is the section inclination Angle, °; β_1 and β_2 are the tectonic stress coefficients in the directions of the maximum and minimum horizontal in-situ stress (dimensionless), respectively, μ is the Poisson's ratio of rock (dimensionless); α is the Biot coefficient (dimensionless), and P_p is the pore fluid pressure, MPa.

3.1.3. Pore-fluid pressure

The mechanical effects of fluids have long been an issue of interest to researchers studying earthquakes and faults (Zoback and Harjes, 1997; Kim, 2013). High pore pressure is a critical factor causing hydraulic fracturing and sliding of pre-existing faults (Luo and Vasseur, 2016). Theoretically, the effective stress acting on a fault mainly depends on the difference between the external stress (fault normal stress) and the pore fluid pressure of the fault rock (Gudehus, 2021). The increase in fluid pressure causes the decrease of rock mechanical strength. Normally, the releasing speed of abnormal shale pressure is much lower than the speed of fault closure process, that is, a fault often re-closes before the shale pressure is significantly reduced. Therefore, the possibility of a fault opening during activity has a positive correlation with the fluid pressure within the shale on both sides of the fault (Wiprut and Zoback, 2000; Zhang et al., 2011). In 1969, Eaton proposed to predict formation pressure using the sonic time difference and the pressure gradient of overburden rock (Eaton, 1969). This method is mature and can acquire formation pressure at different depths using well logging data. It is also commonly used in practical engineering (Eq. (6)).

$$P_p = \sigma_v - (\sigma_v - P_h)\left(\frac{\Delta t_{norm}}{\Delta t}\right) \tag{6}$$

where P_p is the formation pressure, MPa; σ_v is the vertical principal stress, MPa; P_h is the hydro-static pressure at point h, MPa; Δt_{norm} is the acoustic time difference at point h with the change of depth, μs/ft; and Δt is the actual sonic time difference at point h, μs/ft.

3.1.4. Rock brittleness

As the burial depth increases, the physical properties, diagenesis degree, and temperature and pressure environment of the formation change accordingly. As a result, the mechanical properties of shale also change significantly, and there are obvious differences in the degree of brittleness (Fu et al., 2018). Numerous researchers have used sandbox physical simulation and numerical simulation to acquire the fault deformation process of shale layers with different brittleness degrees and the internal structure of fault zones (Vrolijk et al., 2016). The results show that the smear structures caused by different shale brittleness degrees are distinctly different. Under the same degree of fault deformation, ductile shale is susceptible to be distributed along fault zones through smearing. By contrast, brittle shale is prone to fracture, resulting in discontinuous smearing. This kind of shale does not possess the sealing ability (Schmatz et al., 2010; Noorsalehi-Garakani et al., 2013; Kettermann et al., 2017).

At present, there are two pervasively used quantitative evaluation methods for brittleness index. The first one measures the content of brittle minerals, and the second one is the elastic parameter method. For single wells that have undergone array acoustic logging, Young's modulus and Poisson's ratio obtained through rock sonic characteristics are employed to comprehensively characterize the brittleness index. The elastic parameter method can obtain the brittleness index of vertically continuous strata, which is favorable for studying multi-layer systems (Lai et al., 2015). The brittleness index commonly varies between 0 and 1. The closer the value is to 1, the higher the degree of relative brittleness (Richman et al., 2008) (Eqs. (7)–(9)).

$$\mathrm{BI}_E = \frac{E - E_{min}}{E_{max} - E_{min}} \tag{7}$$

$$\mathrm{BI}_\mu = \frac{\mu - \mu_{min}}{\mu_{max} - \mu_{min}} \tag{8}$$

$$\mathrm{BI} = \frac{\mathrm{BI}_E + \mathrm{BI}_\mu}{2} \tag{9}$$

where BI is the brittleness index (dimensionless); E is the Young's modulus of the rock, GPa; μ is the Poisson's ratio of the rock (dimensionless); the subscripts min and max represent the maximum and minimum values of the corresponding parameter within a formation, respectively. BI_E and BI_μ are the brittleness index calculated from Young's modulus and Poisson's ratio, %; respectively.

3.2. Definition of fault transportation index

In summary, the degree of shale smear, stress normal to the fault plane, fluid pressure, and rock brittleness have an important

impact on the vertical transport ability of faults. However, studies that comprehensively considered multiple factors are rare. By analyzing the above influencing factors, we proposed the fault transport index (FTI) to quantitatively characterize the hydrocarbon-transport ability of faults. FTI is defined as the ratio of factors that are beneficial for fault transport to factors hindering fault transport (Eq. (10)).

$$\mathrm{FTI} = \frac{P_\mathrm{p}}{\sigma_\mathrm{N} \cdot \mathrm{SF} \cdot (1 - \mathrm{BI})} \tag{10}$$

where P_p is the fluid pressure, MPa; σ_N is the stress normal to the fault plane, MPa; SF is the smear factor (dimensionless) (shale thickness, fault throw, and shale content are considered in SF), BI is the brittleness index (dimensionless).

In this study, the oil and gas content of the deep and shallow strata near the fault was used to determine whether the fault has transported oil and gas. Taking the F8 fault in Fig. 3 as an example, the strata from the first member of Shahejie Formation to the third member of Dongying Formation are the main source rock of the No. 4 structural zone of the Nanpu Sag. Oil and gas are generated from the source rock and then migrate vertically along the F8 fault. Thus, it can be concluded that the fault segment from the source rock to the shallowest oil and gas layer (points A–E in Fig. 3) is dominated by vertical hydrocarbon transport; otherwise, the cross-layer oil and gas transport cannot be realized. Meanwhile, the fault segment above the shallowest oil and gas layer (point F in Fig. 3) should be vertically closed, preventing the oil and gas from further migration along the fault. Therefore, in Fig. 3, point F is the stop point of oil and gas migration, and point A–E is the oil and gas transport node, which are both effective nodes, while point G cannot reflect whether the fault is connected through the oil and gas show. The above method was used to identify the fault transport ability in the hydrocarbon-source region of the study area, and to perform parameter calculations of fault vertical connectivity.

The vertical transport of oil and gas along faults is affected by a variety of potential factors, and not all fault segments connecting source rocks and oil and gas layers have experienced oil and gas migration. Instead, the actual migration pathways are often complex. Therefore, the FTI obtained only from drilling and profile-interpretation data cannot ensure that each data point is on the hydrocarbon migration path. In the calculation formula of FTI established in this study, we put the factors that promote oil and gas migration along the fault in the denominator and the factors that hinder the transport of oil and gas along the fault in the numerator. We divided the FTI into smaller intervals for statistics to establish the relationship between the FTI and fault vertical transport probability (N_p). N_p is defined as the ratio of the number of oil and gas transport nodes n to the total number of effective nodes N (Eq. (11)):

$$N_\mathrm{p} = n/N \tag{11}$$

4. Results

4.1. Direction and magnitude of stress

Previous studies have shown that the horizontal tensile stress direction in the study area is mainly north-south (Feng et al., 2019; Xu et al., 2019a). In this study, by integrating Eq. (2) with the density logging data, the vertical principal stress magnitude near the PG1 well was obtained (Fig. 4(a) and Eq. (12)). The vertical stress gradient increases from 20.6 to 22.6 Mpa/km as the depth increases. Substituting multiple measured horizontal stress values into Eqs. (3) and (4), β_1 and β_2 were obtained, which show an average value of 0.45 and 0.2, respectively. The horizontal stress interpretation results are described by the sawtooth-shaped line in Fig. 4(a).

$$\sigma_\mathrm{v} = \left(0.0501 \cdot h^2 + 2053.6 \cdot h\right) \cdot 10^{-6} \tag{12}$$

4.2. Characteristics of formation pressure

The fluid pressure calculated using density and acoustic logging data was calibrated by the measured pressure in this study, obtaining a vertically continuous fluid pressure distribution (Fig. 4 (b)). The pressure coefficient (Pc) obtained using the ratio of the formation pressure to hydrostatic pressure at the same depth can reflect whether there is abnormal pressure in the formation. Hao et al. (2005) proposed a pressure classification scheme: strong negative pressure (Pc < 0.8), negative pressure (0.8<Pc < 0.96), normal pressure (0.96<Pc < 1.06), weak overpressure (1.06<Pc < 1.27), overpressure (1.27<Pc < 1.73) and strong overpressure (Pc > 1.73). Taking well PG1 as an example, the strata from the Minghuazhen Formation to the third member of Shahejie Formation is 9.46–58.7 MPa, and the pressure coefficient range is 0.85–1.26, indicative of negative pressure to weak overpressure. The weak overpressure region is mainly distributed in the third member of Dongying Formation and the third member of Shahejie Formation.

4.3. Brittleness index based on elastic parameters

Acoustic logging data and bulk density logs were used to calculate and analyze the rock brittleness index in the study area. Taking Well PG1 as an example, the rock brittleness index at 2900–2970 m is distributed between 0.23 and 0.47 (Fig. 5). In this study, Young's modulus and Poisson's ratio are directly compared with the brittleness index. According to Fig. 5, the higher the Young's modulus and the lower the Poisson's ratio, the larger the rock brittleness.

4.4. Relationship between FTI and fault transportation probability

By determining the layer of vertical fault transport of hydrocarbon and calculating the fault transport index in the No. 4 structural zone, a total of 450 data were obtained. Empirically, the selection of the FTI interval should follow two principles. First, the division range should be small enough. Second, there are enough valid data points in each interval (i.e. $n > 10$). The two principles not only ensure the accuracy of the fitted relationship between the N_p and FTI but also guarantee the statistical sample size of each interval (Zhang et al., 2010, 2011). In this study, according to the two principles, the FTI was divided into 12 intervals, with an increment of 0.25. Based on the statistical analysis of data in each interval (Fig. 6), it is found that when FTI<0.75, the valid data points counted in this interval do not show oil and gas, so N_p equals 0. When FTI>2.5, the data points counted in this interval all have oil and gas displays or oil and gas formations, so N_p equals 1, and when FTI ranges from 0.75 to 2.5, there is a functional relationship between FTI and N_p, with the correlation coefficient being 0.97. Overall, the quantitative relationship between FTI and N_p can be expressed as Eq. (13):

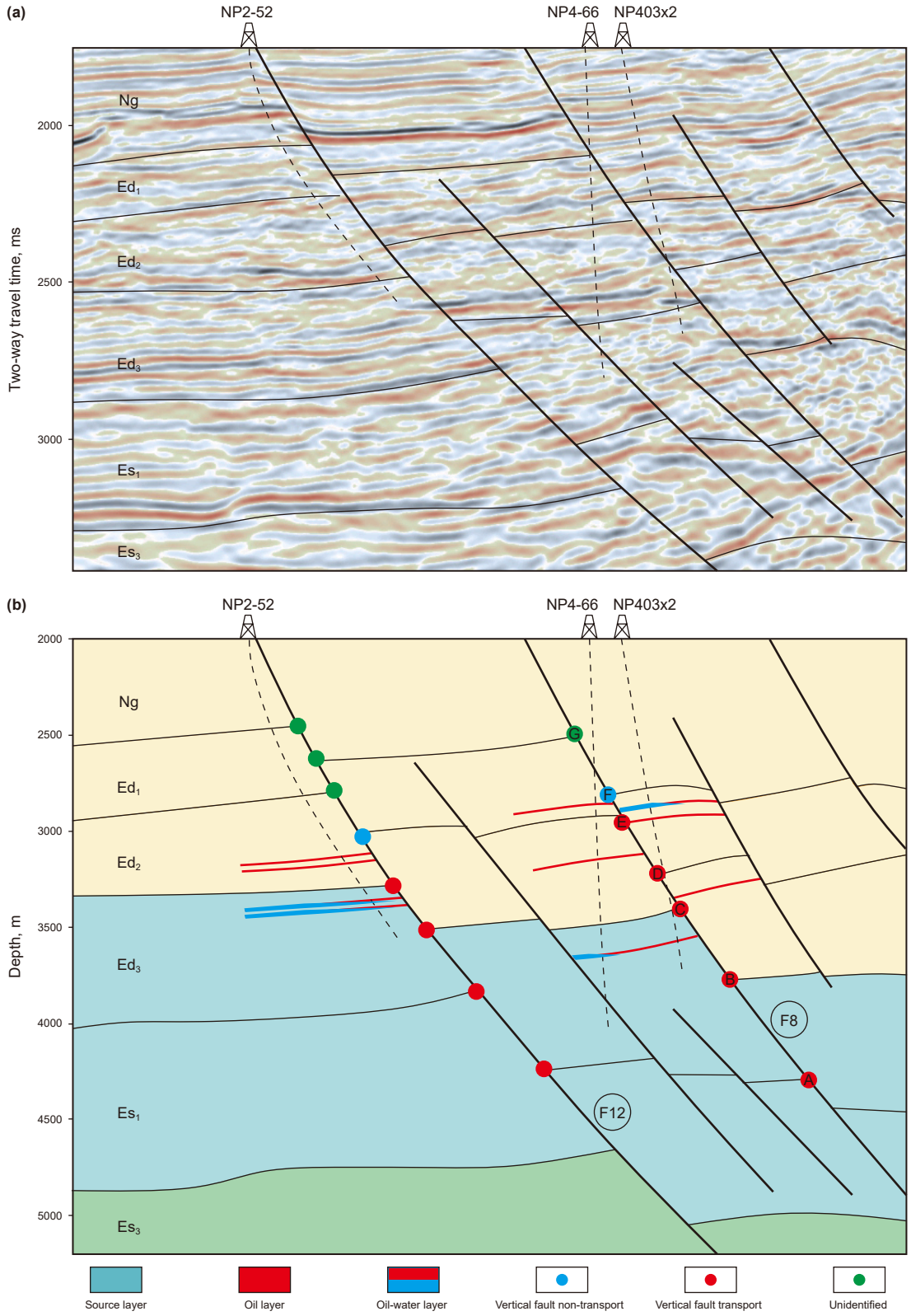

Fig. 3. **(a)** Seismic profile displaying stratigraphic framework and faults. **(b)** Schematic diagram showing the hydrocarbon transportation along F12 and F8 in the No. 4 structural zone in the Nanpu Sag. The location is shown in Fig. 1(b).

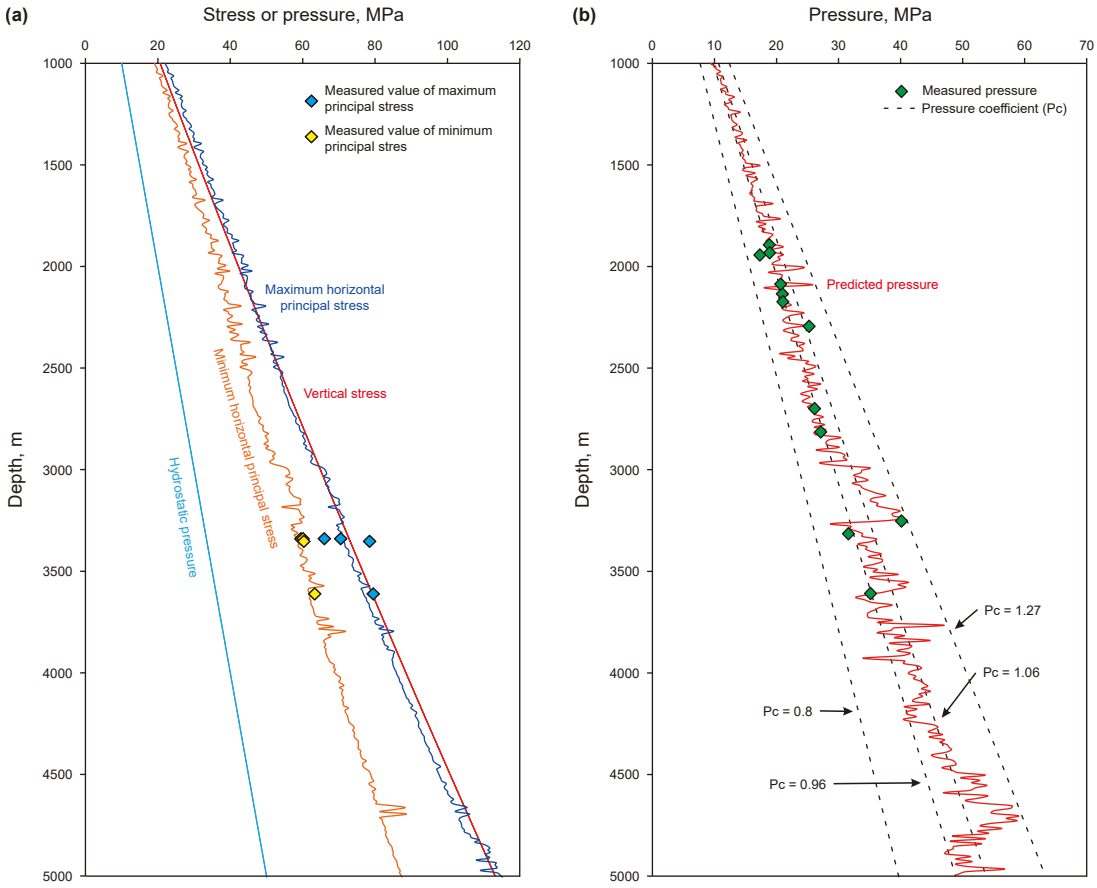

Fig. 4. **(a)** Well (PG1) stress change with depth. **(b)** Well (PG1) formation pressure change with depth.

$$Np = \begin{cases} 0 & FTI \le 0.75 \\ 0.1 \cdot FTI^3 - 0.915 \cdot FTI^2 + 2.67 \cdot FTI - 1.57 & 0.75 < FTI < 2.5 \\ 1 & FTI \ge 2.5 \end{cases} \quad (13)$$

5. Discussion

5.1. Fault transport probability and hydrocarbon distribution

The oil and gas distribution in the study area was analyzed based on the fault transport probability. Taking the F4 fault as an example (Fig. 7), the FTI range from the source rock to the shallowest along-fault reservoir is 1.43–1.78, and the corresponding N_p ranges from 0.69 to 0.88. By contrast, the FTI and N_p above the shallowest reservoir is 0.94 and 0.31, respectively. In statistics, events with a probability greater than 0.5 are called “high probability events”. Specifically, for the F4 fault, the N_p of most of the hydrocarbon-bearing layers is larger than 0.5, but that of the shallowest hydrocarbon without hydrocarbon is less than 0.5. In addition, when calculating the N_p for a single cross-fault profile, we found that some fault segments may not be the effective vertical migration pathways for hydrocarbons. For example, the Nm, Ed_1, and Es_1 formations near the F5 fault (Fig. 7) all have prominent hydrocarbon show, but the N_p in point B of the profile is only 0.41. We further quantitatively characterized of the connection probability along the F5 fault (Fig. 8). The N_p scale indicates the fault transport capacity at different parts of the fault, and the redder the color is, the closer it is to 1, the higher probability the oil and gas will be transported along the fault. It is clear that the N_p changes both horizontally and vertically, demonstrating that oil and gas do not always migrate vertically on the fault plane. When encountering segments with low N_p, oil and gas may migrate laterally over a certain distance and continue to migrate upward at the segments with higher N_p.

Taking the first member of Dongying Formation as an example (Fig. 9(c)), oil and gas are commonly distributed near faults with a high probability of vertical connectivity, which is confirmed by wells NP4-51, NP4-1, NP4-2, etc. Faults that have some segments with a high N_p can also lead to effective hydrocarbon accumulation, such as the locations of wells NP2-53 and NP4-66. However, if the N_p along the entire fault is small, expected hydrocarbon accumulation can hardly occur, such as the location of Well NP2-52. Overall (Fig. 9), F4, F5 and F7 faults have large N_p segments or continuous N_p segments from deep to shallow layers, and oil and gas are enriched in deep and shallow layers. On the north side of the No. 4 structural zone, such as F8, F12 deep layers (bottom interface of the third member of Dongying Formation and the second member of Dongying Formation) have larger N_p, while the N_p near the bottom interface of the first member of Dongying Formation is smaller, preventing oil and gas from migrating to shallow layers. Although the bottom interface of shallow Guantao and Minghuazhen formation have larger N_p, no oil and gas has been found. It should be noted that Fig. 9 only reflects the planar fault transport probability on an interface, and cannot reflect the

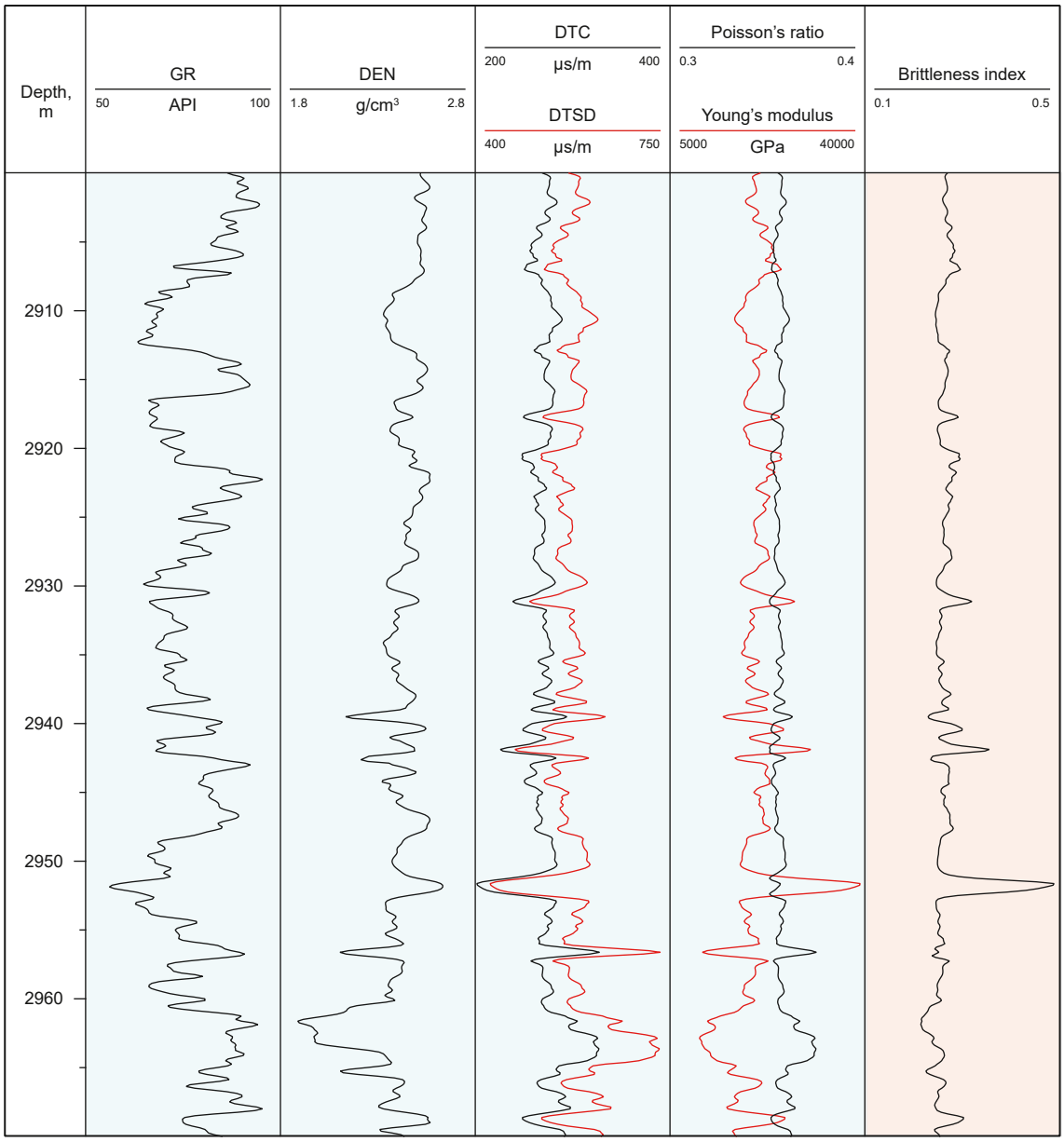

Fig. 5. Calculate the brittleness index of Well PG1 using logging parameters.

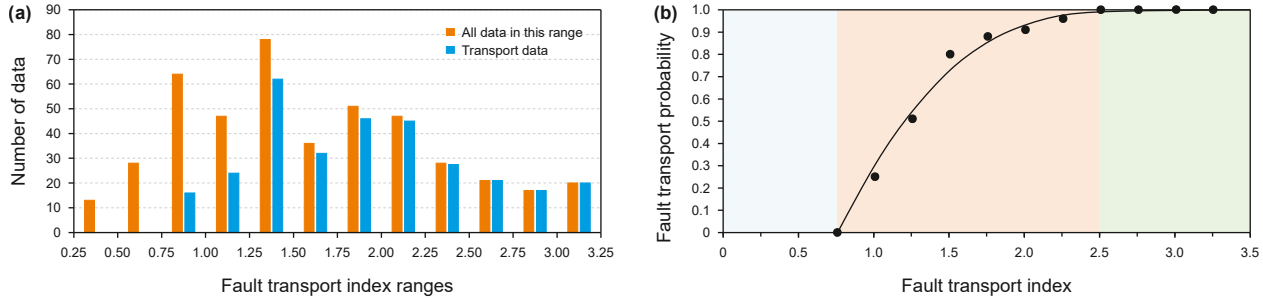

Fig. 6. Relationship curve of the fault transport probability and fault transport index. **(a)** Distribution of the number of total nodes (N) and the number of nodes that served as migration pathways (n) in each statistical range of the fault transport index value. **(b)** Relationship between fault transport probability and fault transport index.

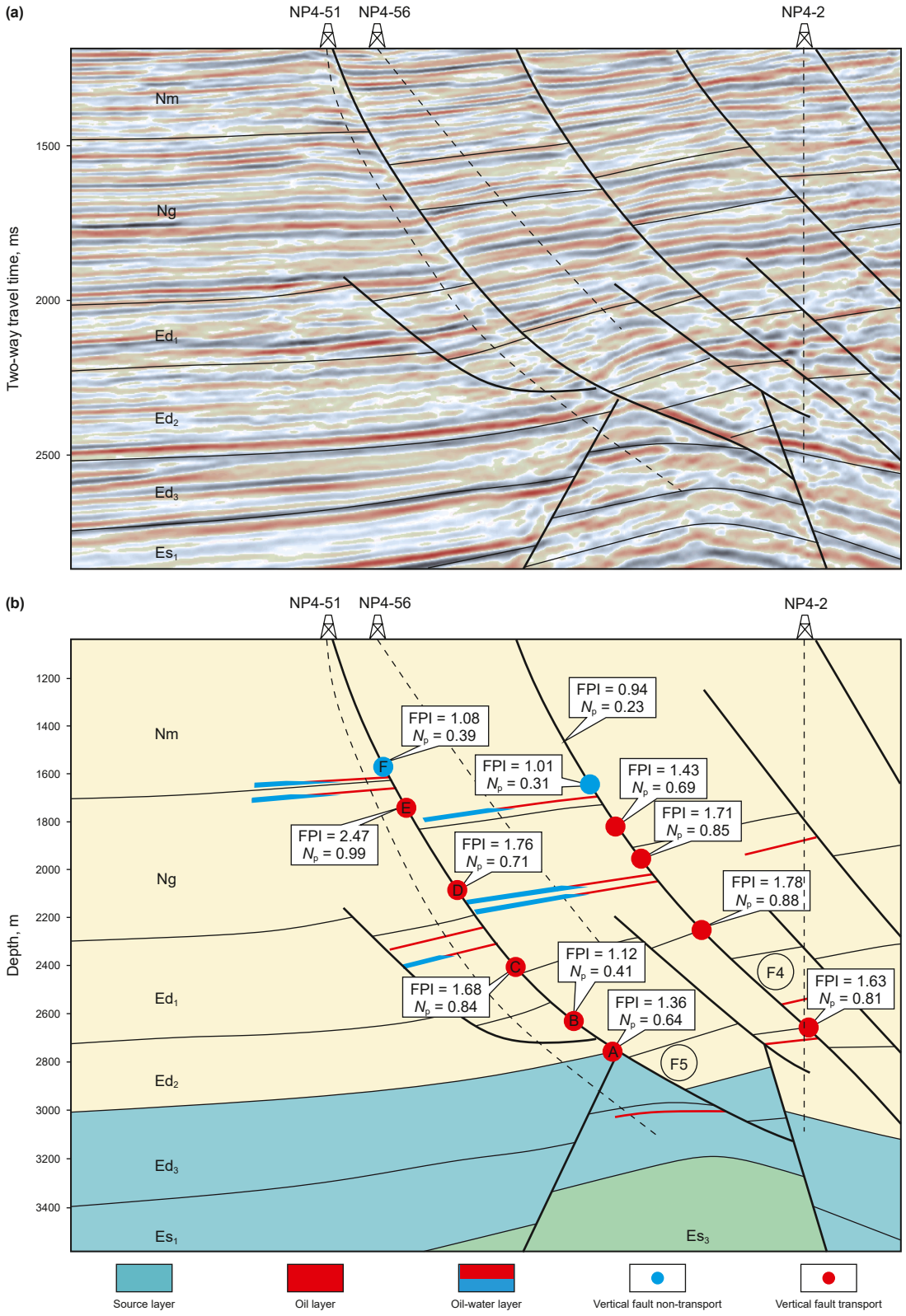

Fig. 7. **(a)** Seismic profile displaying stratigraphic framework and faults. **(b)** Profile traversing wells NP4-51, NP4-56, and NP4-2. The vertical fault transport probability is marked. The location is shown in Fig. 1(b).

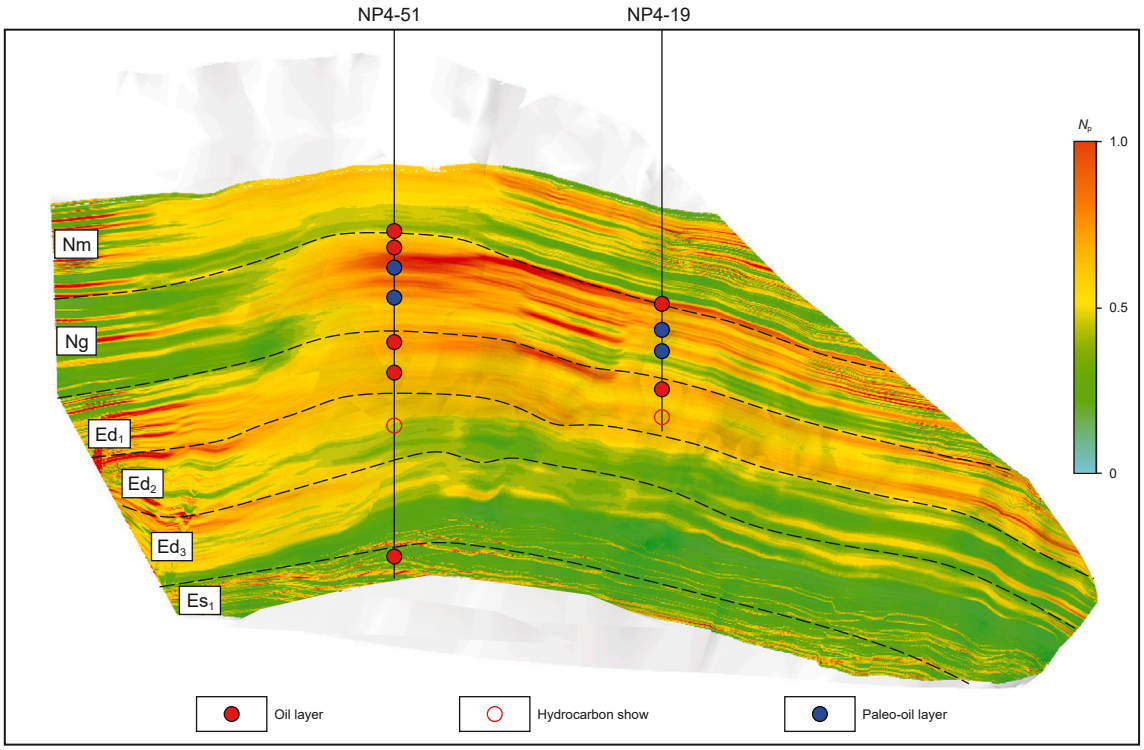

Fig. 8. Fault transport probability (N_p) diagram of the F5 fault plane (Note: The gray shading is the part of the fault plane without N_p data).

entire vertical transport probability along the fault. If the planar fault transport probability is large, the entire vertical transport probability may not be large. However, if the planar N_p is small, oil and gas can hardly migrate along the correspond fault.

We conducted paleo-reservoir testing on water layers with a high N_p, aiming to prove that oil and gas indeed migrate along areas with a higher fault transport probability. Quantitative grain fluorescence (QGF) of reservoirs is an effective means to identify the paleo and current oil-water interfaces, restore the evolution history of oil and gas reservoirs, and determine the migration pathways of oil and gas. The QGF index of paleo oil layers are generally greater than 4, while that of paleo water layers is generally less than 4; the quantitative grain fluorescence intensity of reservoir extracts of current oil layers is basically greater than 40 pc, while that of water layer samples is generally less than 20 pc (Liu et al., 2007). Taking wells NP4-19 and NP4-51 as examples, it was found that oil and gas are enriched near the top of Ng. However, although the FTI in the middle part of Ng is large, this region is currently a water layer. Performing paleo oil reservoir testing on the water layer samples from the middle part of Ng, we found that the QGF indexes of the samples at depths of 2318 m and 2343 m in Well NP4-19 and the samples at depths of 1862 m and 1905 m in Well NP4-51 are greater than 4 (Table 1). In addition, the QGF spectrum has obvious peaks at 350–400 nm (Fig. 10), indicating a paleo oil reservoir at this depth, and oil and gas have vertically migrated in the region with a high N_p along the fault.

5.2. Reservoir formation mode controlled by the vertical fault transport ability

Highly developed faults are important vertical hydrocarbon transport channels and are also the critical prerequisite for the enrichment of multi-layered oil and gas in the Nanpu Sag. Influenced by the inherited development of structural zones, strong tectonic movements in the late period produced numerous faults connecting the source rocks, creating favorable conditions for oil and gas to migrate toward shallower layers. However, not all faults connecting with the source rocks are able to transport oil and gas to shallow layers. Whether a fault can transport oil and gas and which layers can the oil and gas reach depend on the vertical fault transport ability, which can be quantitatively characterized by N_p. In locations with an N_p greater than 0.5, oil and gas are more likely to migrate vertically along the fault. By investigating the shallow hydrocarbon migration and accumulation process in the No. 4 structural zone of the Nanpu Sag, it was found that the oil and gas generated from the main source rocks, which were determined to be the first member of Shahejie Formation and the third member of Dongying Formation (Gao et al., 2021), have extensively migrated along faults and accumulated in shallow layers since the late Minghuazhen period. Affected by the vertical transport capacity of faults, the layers that oil and gas can reach along different faults are different. For example, the Es_1 and Ed_3 formations near the F12 fault have a higher N_p, and thus the oil and gas can migrate vertically to the lower part of Ed_2 (Fig. 11). However, the N_p in the upper part of Ed_2 is small, preventing the further migration of oil and gas (Fig. 11). Although the N_p becomes higher again the fault segment within the Ng layer, the upper parts of Ed_1 and Ed_2 formations (with a small N_p) act as barriers. Thus, oil and gas cannot migrate to Ng through the F12 fault. By comparison, the F4 and F5 faults have vertical transport probabilities greater than 0.5 from Es_1 to the bottom of Nm, and are thus considered as effective faults that can transport deep hydrocarbons to the shallow layers. As a result, oil and gas reservoirs are discovered in multiple formations near the fault F4 and F5 (Fig. 10). In addition, the paleo-reservoir test has shown that the oil and gas migration and accumulation along faults are multi-episodic. For example, there are paleo-reservoirs in Ng of well NP4-19, Ng and Ed_1 of well NP4-51, and Ed_3 of well NP4-66 (Table 1), and oil and gas accumulations exist in

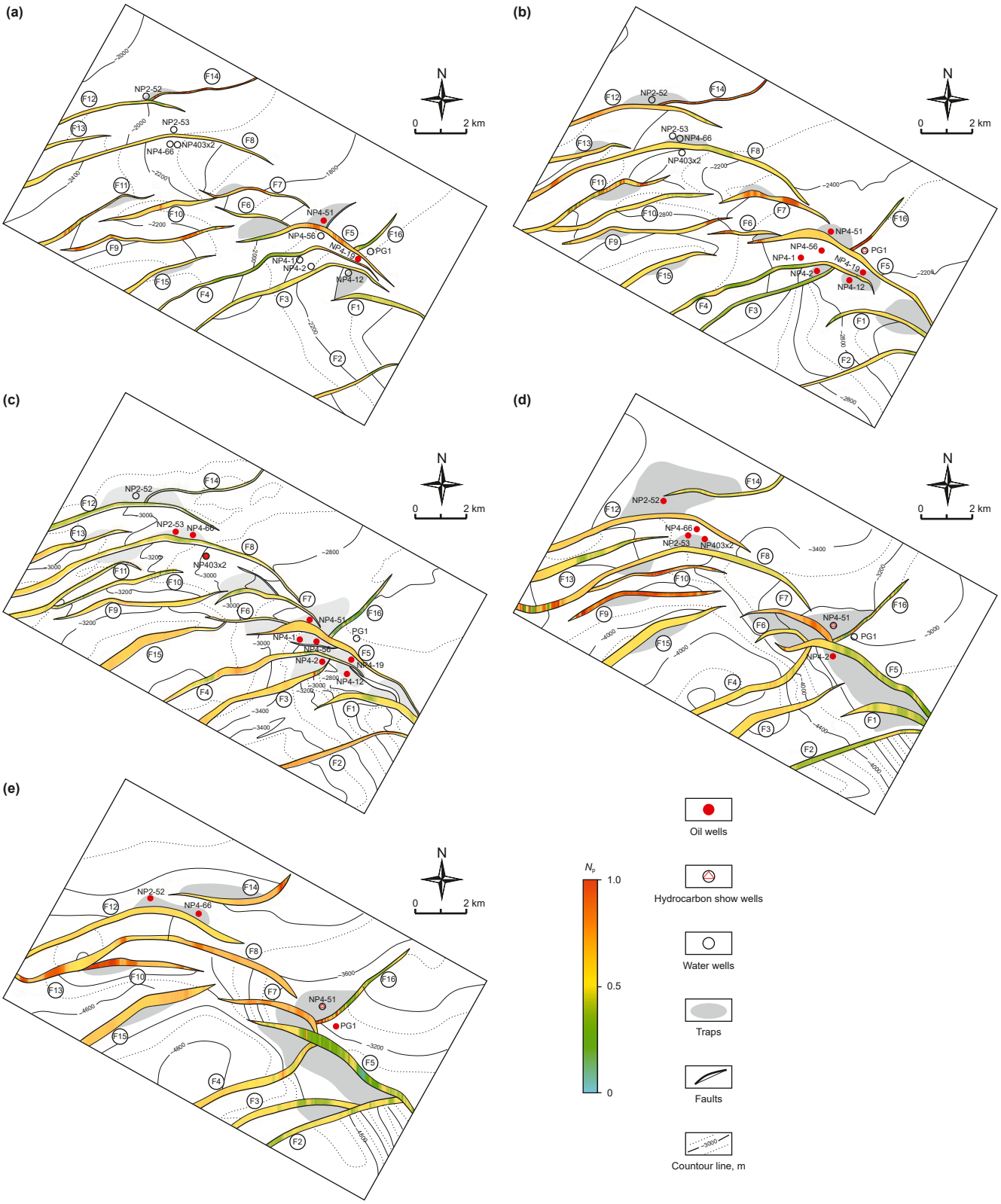

Fig. 9. Fault transport probability (N_p) of major faults and hydrocarbon display. **(a)** Bottom interface of Minghuazhen Formation. **(b)** Bottom interface of Guantao Formation. **(c)** Bottom interface of the first member of Dongying Formation. **(d)** Bottom interface of the second member of Dongying Formation. **(e)** Bottom interface of the third member of Dongying Formation.

Table 1
Quantitative fluorescene test results of the reservoir grains in the Nanpu Sag.

Well number	Depth, m	Layer	QGF index	QGF-E intensity, pc
NP4-19	2318	Ng	7.3	332
NP4-19	2343	Ng	4	96.8
NP4-19	2381	Ng	3.6	7518.3
NP4-51	1862	Ng	5.2	208.4
NP4-51	1905	Ng	4.9	538.5
NP4-51	2632	Ed_1	3.3	244.1
NP4-66	3695	Ed_3	5.3	1282.3
NP4-66	3760	Ed_3	4.7	2514.1
NP4-66	3815	Ed_3	5.2	2492.8
NP4-66	3880	Ed_3	4.9	920.1
NP4-66	3890	Ed_3	6.2	2684

the shallow layers above these paleo reservoirs (Figs. 3 and 11). Such a phenomenon shows that during the geological process, oil and gas have accumulated or stayed shortly in paleo oil reservoirs, and the later fault activity migrated oil and gas to shallow layers. Based on the above evaluation results and fault transport probability, we suggest that F4, F5, F6, F7, F9, F15 in the No. 4 structural zone have high probability to transport hydrocarbons continuously from deep layers to shallow layers.

Most previous studies regarding fault-controlled hydrocarbon migration focused on the hydrocarbon enrichment near the caprock layer and often ignored hydrocarbon migration and accumulation in other formations (e.g. Yielding et al., 1997; Lv et al., 2007; Fu et al., 2018), and some studies considered only a single geological factor or few factors (Xu et al., 2019b; Foschi and

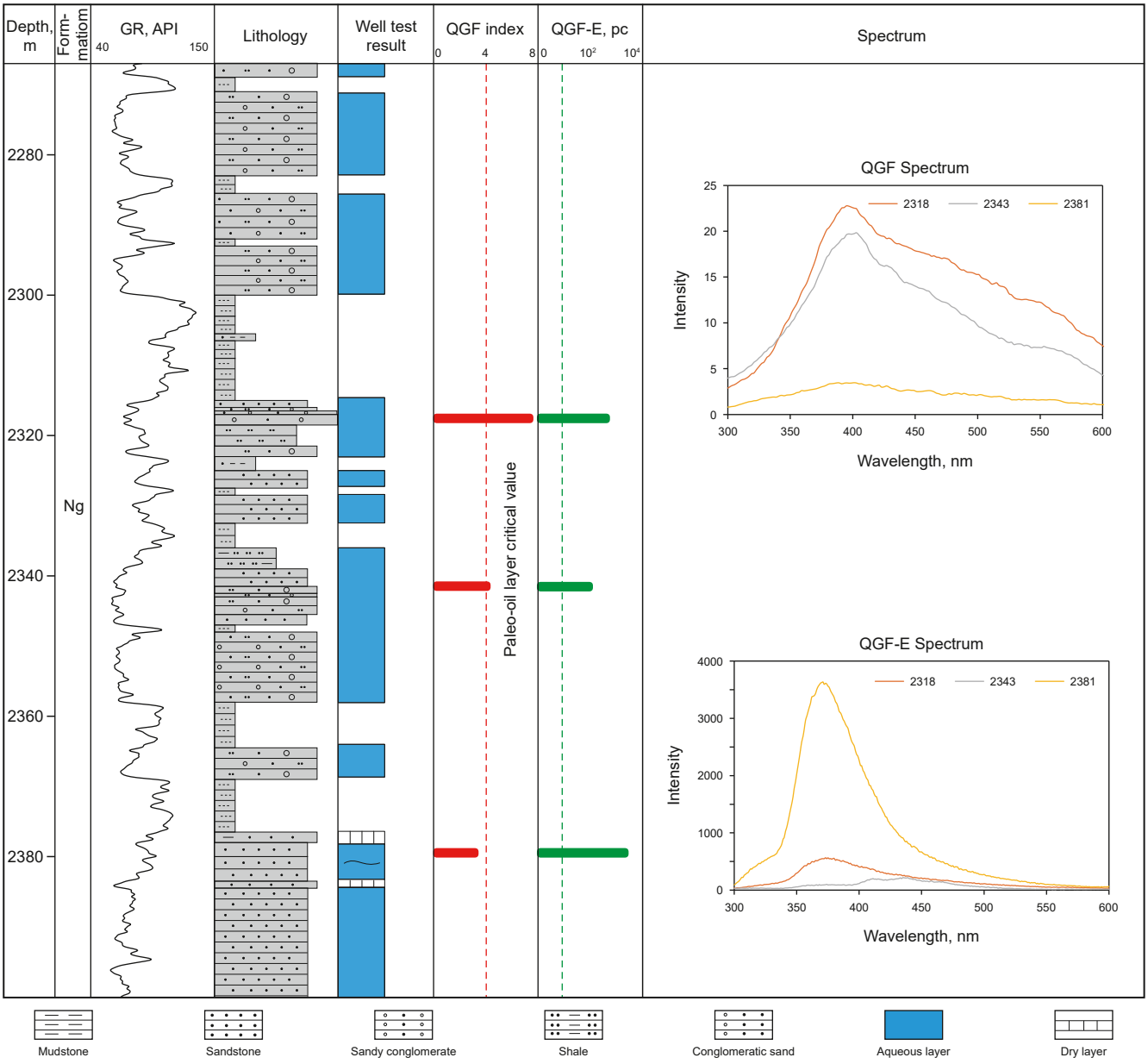

Fig. 10. Quantitative Grain Fluorescene (QGF) identification results of Well NP4-19.

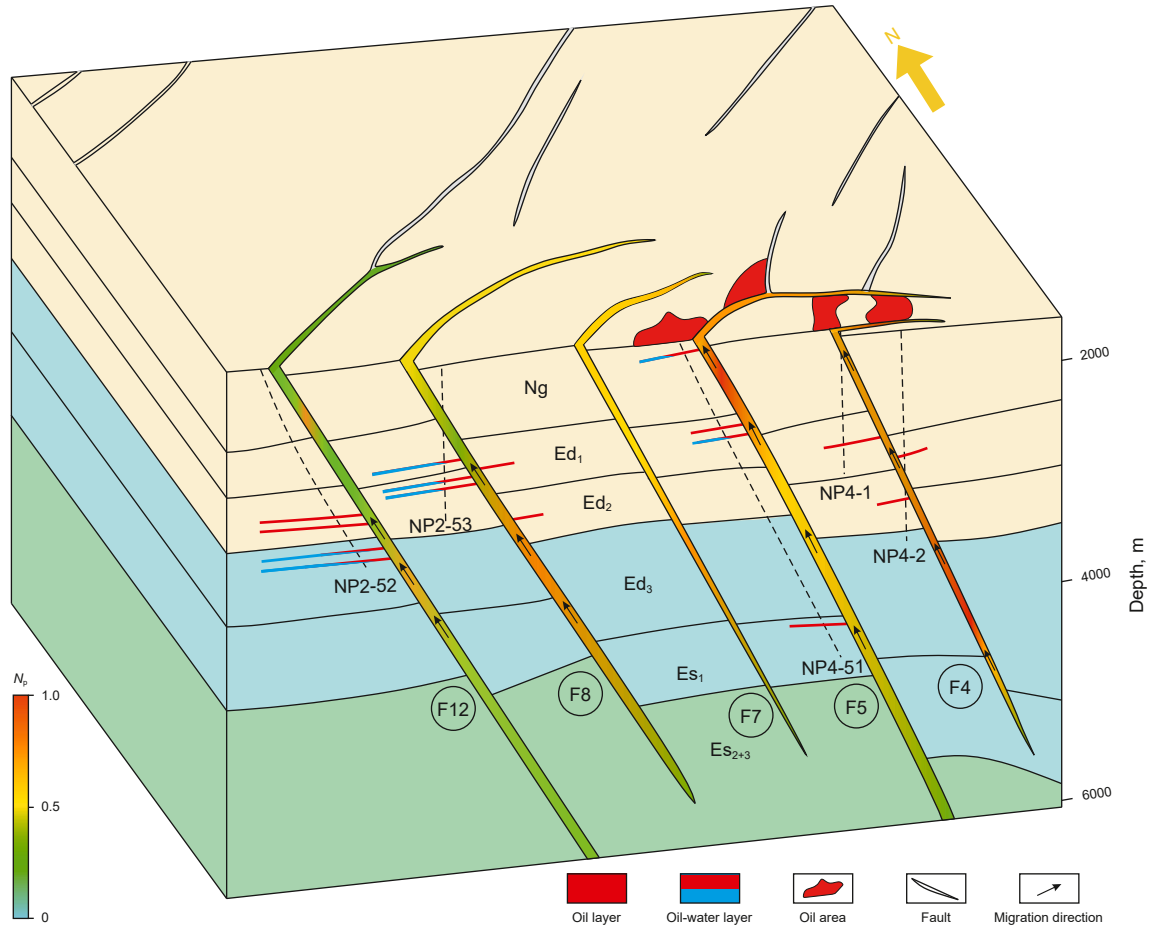

Fig. 11. Reservoir formation mode of the No. 4 structural zone in the Nanpu Sag.

Van, 2022; Allgaier et al., 2023). Compared to these studies, this study investigated multiple geological factors in the study area, quantitatively characterized faults' transport ability by establishing significant parameters such as FTI and N_p, and successfully predicted the along-fault hydrocarbon transport pathways and enrichment layers. In addition to the factors mentioned in this article, there are many other possible influencing factors, such as the properties of hydrocarbons (e.g. density, viscosity, phase state, etc.), temperature, mineralization degree, etc. In this study, we considered all the factors that have a clear correlation with the vertical hydrocarbon migration in our quantitative fault evaluation system. How to decipher the contribution of each factor may be the key to further investigating the process of vertical migration of oil and gas along faults.

6. Conclusions

Faults are highly developed in the No. 4 structural zone of the Nanpu Sag, serving as essential channels for vertical oil and gas migration, which is the significant prerequisite for the multi-layer hydrocarbon enrichment in this region. Hydrocarbons migration and accumulation along faults are multi-episodic. Whether hydrocarbons can migrate from source rock to shallow layers depends on faults' transport ability. In this study, fault transport index (FTI) was proposed to quantify the vertical transport ability of faults in the No. 4 structural zone. When FTI<0.75, faults are not able to transport oil and gas; when FTI>2.5, faults can transport oil and gas; when 0.75<FTI<2.5, there is a functional relationship between FTI and vertical fault transport probability (N_p), with a correlation coefficient of 0.97. In regions with an N_p greater than 0.5, hydrocarbons are more likely to migrate vertically along faults, and some faults (F4, F5, F6, F7, F9, F15) in the No. 4 structural zone have high probability to transport hydrocarbons continuously from deep layers to shallow layers.

CRediT authorship contribution statement

Xiao-Fei Fu: Writing – review & editing, Conceptualization. **Ming-Xing Fan:** Writing – original draft, Conceptualization. **Hai-Xue Wang:** Validation, Methodology. **Ru Jia:** Visualization, Data curation. **Xian-Qiang Song:** Visualization, Data curation. **Ye-Jun Jin:** Visualization, Data curation.

Declaration of competing interest

The authors declare that they have no known competing financial interests or personal relationships that could have appeared to influence the work reported in this paper.

Acknowledgements

This research was financially supported by the National Natural Science Foundation of China (Grant Nos. 42302150 and U20A2093), and National Science and Technology Major Project (Grant No. 2024ZD1400104).

References

Allgaier, F., Busch, B., Hilgers, C., 2023. Fault leakage and reservoir charging in the upper Rhine Graben, Germany-Assessment of the Leopoldshafen fault bend. Mar. Petrol. Geol. 156, 106428. https://doi.org/10.1016/j.marpetgeo.2023.106428.

Anders, M.H., Schlische, R.W., 1994. Overlapping faults, intrabasin highs, and the growth of normal faults. J. Geol. 102 (2), 165–179. https://doi.org/10.1086/629661.

Berg, R.R., Avery, A.H., 1995. Sealing properties of tertiary growth faults, Texas Gulf Coast. AAPG Bull. 79 (3), 375–392. https://doi.org/10.1306/8D2B1534-171E-11D7-8645000102C1865D.

Berg, S.S., Skar, T., 2005. Controls on damage zone asymmetry of a normal fault zone: Outcrop analyses of a segment of the Moab Fault, SE Utah. J. Struct. Geol. 27 (10), 1803–1822. https://doi.org/10.1016/j.jsg.2005.04.012.

Bruhn, R.L., Yonkee, W.A., Parry, W.T., 1990. Structural and fluid-chemical properties of seismogenic normal faults. Tectonophysics 175 (1–3), 139–157. https://doi.org/10.1016/0040-1951(90)90135-u.

Caine, J.S., Evans, J.P., Forster, C.B., 1996. Fault zone architecture and permeability structure. Geology 24 (11), 1025–1028. https://doi.org/10.1130/0091-7613(1996)024<1025:fzaaps>2.3.co.

Clausen, J.A., Gabrielsen, R.H., 2002. Parameters that control the development of clay smear at low stress states: An experimental study using ring-shear apparatus. J. Struct. Geol. 24 (10), 1569–1586. https://doi.org/10.1016/s0191-8141(01)00157-2.

Eaton, B.A., 1969. Fracture gradient prediction and its application in oilfield operations. J. Petrol. Technol. 21 (10), 1353–1360. https://doi.org/10.2118/2163-PA.

Evans, M.A., Ferrill, D.A., Smart, K.J., 2024. Evidence for regional fluid migration in the Eagle Ford Formation, Austin Chalk, and Buda Limestone of south-central and west Texas, USA. Mar. Petrol. Geol. 166, 106896. https://doi.org/10.1016/j.marpetgeo.2024.106896.

Fan, M.X., Wang, H.X., Fu, X.F., et al., 2023. Oil source and accumulation mechanism of the Damoguaihe Formation in the Southern Wuerxun Sag, Hailaer Basin. China. Mar. Petrol. Geol. 153, 106266. https://doi.org/10.1016/j.marpetgeo.2023.106266.

Feng, J.W., Shang, L., Li, X.Z., et al., 2019. 3D numerical simulation of heterogeneous *in situ* stress field in low-permeability reservoirs. Pet. Sci. 16, 939–955. https://doi.org/10.1007/s12182-019-00360-w.

Foschi, M., Van Rensbergen, P., 2022. Topseal integrity assessment using seal properties and leakage phenomena. Mar. Petrol. Geol. 139, 105573. https://doi.org/10.1016/j.marpetgeo.2022.105573.

Fu, X.F., Song, X.Q., Wang, H.X., et al., 2021. Comprehensive evaluation on hydrocarbon-bearing availability of fault traps in a rift basin: A case study of the Qikou Sag in the Bohai Bay Basin, China. Petrol. Explor. Dev. 48 (4), 787–797. https://doi.org/10.1016/S1876-3804(21)60066-6.

Fu, X.F., Wu, T., Lyu, Y.F., et al., 2018. Research status and development trend of the reservoir caprock sealing properties. Oil Gas Geol. 39 (3), 454–471. https://doi.org/10.11743/ogg20180304 (in Chinese).

Gao, G., Zhao, J.Y., Yang, S.R., et al., 2021. Characteristics and origin of oil and gas in the Nanpu Sag, Bohai Bay Basin, China: Insights from oil-source correlation and source rock effects. AAPG Bull. 105 (7), 1435–1460. https://doi.org/10.1306/01152117395.

Giger, S.B., Clennell, M.B., Ciftci, N.B., et al., 2013. Fault transmissibility in clastic-argillaceous sequences controlled by clay smear evolution. AAPG Bull. 97 (5), 705–731. https://doi.org/10.1306/10161211190.

Gudehus, G., 2021. Implications of the principle of effective stress. Acta Geotech 16 (6), 1939–1947. https://doi.org/10.1007/s11440-020-01068-7.

Gudmundsson, A., 2001. Fluid Overpressure and flow in fault zones: field measurements and models. Tectonophysics 336 (1–4), 183–197. https://doi.org/10.1016/s0040-1951(01)00101-9.

Haney, M.M., Snieder, R., Sheiman, J., et al., 2005. A moving fluid pulse in a fault zone. Nature 437 (7055), 46. https://doi.org/10.1038/437046a.

Hao, F., Jin, Z.J., Zou, H.Y., 2005. Kinetics of Hydrocarbon Generation and Mechanisms of Petroleum Accumulation in Overpressured Basins. Science Press, Beijing, pp. 76–96 (in Chinese).

Harding, T.P., Tuminas, A.C., 1989. Structural interpretation of hydrocarbon traps sealed by basement normal block faults at stable flank of foredeep basins and at rift basins. AAPG Bull. 73 (7), 812–840. https://doi.org/10.1306/44B4A276-170A-11D7-8645000102C1865D.

Hooper, E., 1991. Fluid migration along growth faults in compacting sediments. J. Petrol. Geol. 14, 161–180. https://doi.org/10.1111/j.1747-5457.1991.tb00360.x.

Huang, R.Z., 1984. A model for predicting formation fracture pressure. J. Univ. Pet., China (Ed. Nat. Sci.) 26 (4), 335–347 (in Chinese).

Im, K., Elsworth, D., Fang, Y., 2018. The influence of preslip sealing on the permeability evolution of fractures and faults. Geophys. Res. Lett. 45, 166–175. https://doi.org/10.1002/2017GL076216.

Jaeger, J.C., Cook, N.G., Zimmerman, R., 2009. Fundamentals of Rock Mechanics. Wiley-Blackwell, Oxford. https://doi.org/10.1016/0040-1951(77)90223-2.

Jiang, F.J., Pang, X.Q., Li, L.L., et al., 2018. Petroleum resources in the Nanpu Sag, Bohai Bay Basin, Eastern China. AAPG Bull. 102 (7), 1213–1237. https://doi.org/10.1306/0906171608017148.

Jiang, M.M., Fu, X.F., Wang, Z.C., et al., 2024. An experimental investigation of the characteristics of cataclastic bands in high-porosity sandstones. Geol. Soc. Am. Bull. 136 (7–8), 3069–3084.

Jiang, M.M., Jin, Y.J., Fu, X.F., et al., 2023. The development of cataclastic bands in high-porosity sandstones: insights from ring shear experiments. J. Struct. Geol. 175, 104952. https://doi.org/10.1016/j.jsg.2023.104952.

Jiang, Y.L., Su, S.M., Zhao, K., 2022. Relationship between transporting ability of oil-source faults and hydrocarbon enrichment in non-hydrocarbon generating strata: A case study of Chengdao Area of Bohai Bay Basin. Acta Pet. Sin. 43 (8), 1122–1131. https://doi.org/10.7623/syxb202208007 (in Chinese).

Jin, Y.J., Meng, L.D., Lyu, D.Y., et al., 2023. Risk assessment of fault reactivation considering the heterogeneity of friction strength in the BZ34-2 Oilfield, Huanghekou Sag, Bohai Bay Basin, China. Pet. Sci. 20 (5), 2695–2708. https://doi.org/10.1016/j.petsci.2023.06.007.

Jones, R.M., Hillis, R.R., 2003. An integrated, quantitative approach to assessing fault-seal risk. AAPG Bull. 87 (3), 507–524. https://doi.org/10.1306/10100201135.

Kettermann, M., Urai, J.L., Vrolijk, P.J., 2017. Evolution of structure and permeability of normal faults with clay smear: insights from water-saturated sandbox models and numerical simulations. J. Geophys. Res. Solid Earth 122 (3), 1697–1725. https://doi.org/10.1002/2016jb013341.

Kim, W.Y., 2013. Induced seismicity associated with fluid injection into a deep well in Youngstown, Ohio. J. Geophys. Res. Solid Earth 118 (7), 3506–3518. https://doi.org/10.1002/jgrb.50247.

Knipe, R.J., 1997. Juxtaposition and seal diagrams to help analyze fault seals in hydrocarbon reservoirs. AAPG Bull. 81 (2), 187–195. https://doi.org/10.1306/522B42DF-1727-11D7-8645000102C1865D.

Lai, J., Wang, G., Huang, L., et al., 2015. Brittleness index estimation in a tight shaly sandstone reservoir using well logs. J. Nat. Gas Sci. Eng. 27, 1536–1545. https://doi.org/10.1016/j.jngse.2015.10.020.

Li, S.M., Pang, X.Q., Wan, Z.H., 2011. Mixed oil distribution and source rock discrimination of the Napu Depression, Bohaibay Basin. Earth Sci. (J. China Univ. Geosci.) 36 (6), 1064–1072 (in Chinese).

Liu, L., Sun, Y.H., Chen, C., et al., 2022. Fault reactivation in No. 4 structural zone and its control on oil and gas accumulation in Nanpu Sag. Petrol. Explor. Dev. 49 (4), 824–836. https://doi.org/10.11698/PED.20220056.

Liu, H., Ouyang, G.Y., Liu, X., et al., 2024. Characteristics of oil-source faults and differential enrichment patterns of oil and gas in Nanpu Sag in Bohai Bay Basin. Petrol. Geol. Oilfield Dev. Daqing. 2024 43 (5), 1–12. https://doi.org/10.19597/J.ISSN.1000-3754.202303033 (in Chinese).

Liu, K.Y., Eadington, P., Middleton, H., et al., 2007. Applying quantitative fluorescence techniques to investigate petroleum charge history of sedimentary basins in Australia and Papuan New Guinea. J. Petrol. Sci. Eng. 57 (1–2), 139–151. https://doi.org/10.1016/j.petrol.2005.11.019.

Luo, X.R., Vasseur, G., 2016. Overpressure dissipation mechanisms in sedimentary sections consisting of alternating mud-sand layers. Mar. Petrol. Geol. 78, 883–894. https://doi.org/10.1016/j.marpetgeo.2016.04.001.

Lv, D.Y., Huang, Z., Yang, H.F., et al., 2022. Controlling effect of tectonic deformation unit on vertical hydrocarbon migration and its exploration significance: A case study of neogene oil and gas exploration in Circum-Bozhong Sag, Bohai Bay Basin. Acta Pet. Sin. 43 (8), 1078–1088. https://doi.org/10.7623/syxb202208004 (in Chinese).

Lv, Y.F., Li, G.H., Wang, Y.W., et al., 1996. Quantitative analyses in fault sealing properties. Acta Pet. Sin. 3, 39–45. https://doi.org/10.7623/syxb199603006 (in Chinese).

Lv, Y.F., Sha, Z.X., Fu, X.F., et al., 2007. Quantitative evaluation method for fault vertical sealing ability and its application. Acta Pet. Sin. (5), 34–38. https://doi.org/10.7623/syxb200705006 (in Chinese).

Lv, Y.F., Wei, D.N., Sun, Y.H., et al., 2015. Control action of faults on hydrocarbon migration and accumulation in the middle and upper oil-bearing group in Nanpu Sag. J. Jilin Univ. (Earth Sci. Ed.) 45 (4), 971–982. https://doi.org/10.13278/j.cnki.jjuese.201504101 (in Chinese).

Noorsalehi-Garakani, S., Vennekate, G.K., Vrolijk, P., et al., 2013. Clay-smear continuity and normal fault zone geometry-first results from excavated sandbox models. J. Struct. Geol. 57, 58–80. https://doi.org/10.1016/j.jsg.2013.09.008.

Pang, B., Dong, Y.X., Chen, D., et al., 2019. Main controlling factors and basic model for hydrocarbon enrichment in the sandstone target layer of petroliferous basin: A case study of neogenesandstone reservoirs in Nanpu Sag, Bohai Bay Basin. Acta Pet. Sin. 40 (5), 519–531. https://doi.org/10.7623/syxb201905002.

Rickman, R., Mullen, M., Petre, E., et al., 2008. A practical use of shale petrophysics for stimulation design optimization: all shale plays are not clones of the Barnett shale. In: SPE Annual Technical Conference and Exhibition?. https://doi.org/10.2118/115258-MS.

Ryan, L., Magee, C., Jackson, C.A.L., 2017. The kinematics of normal faults in the Ceduna Subbasin, offshore southern Australia: implications for hydrocarbon trapping in a frontier basin. AAPG (Am. Assoc. Pet. Geol.) Bull. 101 (3), 321. https://doi.org/10.1306/08051615234.

Schmatz, J., Vrolijk, P.J., Urai, J.L., 2010. Clay smear in normal fault zones-the effect of multilayers and clay cementation in water-saturated model experiments. J. Struct. Geol. 32 (11), 1834–1849. https://doi.org/10.1016/j.jsg.2009.12.006.

Sibson, R.H., Moore, J.M.M., Rankin, A.H., 1975. Seismic pumping-a hydrothermal fluid transport mechanism. J. Geol. Soc. London 131 (6), 653–659. https://doi.org/10.1144/gsjgs.131.6.0653.

Smeraglia, L., Fabbi, S., Billi, A., et al., 2022. How hydrocarbons move along faults: evidence from microstructural observations of hydrocarbon-bearing carbonate fault rocks. Earth Planet Sci. Lett. 584, 117454. https://doi.org/10.1016/j.epsl.2022.117454.

Song, X.Q., Wang, H.X., Fu, X.F., et al., 2022. Hydrocarbon retention and leakage in traps bounded by active faults: a case study from traps along the NDG fault in the qinan area, Bohai Bay Basin, China. J. Petrol. Sci. Eng. 208, 109344. https://doi.org/10.1016/j.petrol.2021.109344.

Sperrevik, S., Færseth, R.B., Gabrielsen, R.H., 2000. Experiments on clay smear formation along faults. Pet. Geosci. 6 (2), 113–123. https://doi.org/10.1144/petgeo.6.2.113.

Tong, H.M., Zhao, B.Y., Chao, Z., et al., 2013. Structural analysis of faulting system origin in the Nanpu Sag, Bohai Bay Basin. Acta Geol. Sin. 87 (11), 1647–1661. https://doi.org/10.19762/j.cnki.dizhixuebao.2013.11.002.

Vrolijk, P.J., Urai, J.L., Kettermann, M., 2016. Clay smear: review of mechanisms and applications. J. Struct. Geol. 86, 95–152. https://doi.org/10.1016/j.jsg.2015.09.006.

Wan, T., Jiang, Y.L., Dong, Y.X., et al., 2013. Reconstructed and traced pathways of hydrocarbon migration in Nanpu Depression, Bohai Bay Basin. Earth Sci. 38 (1), 173–180.

Wang, K., Dai, J.S., 2012. A quantitative relationship between the crustal stress and fault sealing ability. Acta Pet. Sin. 33 (1), 74–81. https://doi.org/10.7623/syxb201201009.

Wang, W.Y., Pang, X.Q., Chen, Z.X., et al., 2021. Quantitative evaluation of transport efficiency of fault-reservoir composite migration pathway systems in carbonate petroliferous basins. Energy 222, 119983. https://doi.org/10.1016/j.energy.2021.119983.

Wang, Z.C., Zheng, H.J., Xu, A.N., et al., 2008. Oil-gas exploration potential for above-source plays in Nanpu Sag. Petrol. Explor. Dev. 35 (1), 11–16. https://doi.org/10.1016/S1876-3804(08)60003-8.

Wiprut, D., Zoback, M.D., 2000. Fault reactivation and fluid flow along a previously dormant normal fault in the Northern North Sea. Geology 28 (7), 595–598. https://doi.org/10.1130/0091-7613(2000)28<595:fraffa>2.0.co.

Xu, K., Dai, J.S., Shang, L., et al., 2019a. Characteristics and influencing factors of in-situ stress of Nanpu Sag, Bohai Bay Basin, China. J. China Inst. Min. Technol. 48 (3), 570–583. https://doi.org/10.13247/j.cnki.jcumt.000937 (in Chinese).

Xu, S., Hao, F., Xu, C.G., et al., 2019b. Hydrocarbon migration and accumulation in the northwestern Bozhong Subbasin, Bohai Bay Basin, China. J. Petrol. Sci. Eng. 172, 477–488. https://doi.org/10.1016/j.petrol.2018.09.084.

Yielding, G., 2002. Shale gouge ratio-calibration by geohistory. Norweg. Petrol. Soc. Spec. Publ. 11 (2), 1–15. https://doi.org/10.1016/S0928-8937(02)80003-0.

Yielding, G., Freeman, B., Needham, D.T., 1997. Quantitative fault seal prediction. AAPG Bull. 81 (6), 897–917. https://doi.org/10.1002/(SICI)1099-114X(19970610)21:7<675::AID-ER287>3.0.CO;2-Z.

Zhang, L.K., Luo, X.R., Liao, Q.J., et al., 2010. Quantitative evaluation of synsedimentary fault opening and sealing properties using hydrocarbon connection probability assessment. AAPG Bull. 94 (9), 1379–1399. https://doi.org/10.1306/12140909115.

Zhang, L.K., Luo, X.R., Vasseur, G., et al., 2011. Evaluation of geological factors in characterizing fault connectivity during hydrocarbon migration: Application to the Bohai Bay Basin. Mar. Petrol. Geol. 28 (9), 1634–1647. https://doi.org/10.1016/j.marpetgeo.2011.06.008.

Zhu, G.Y., Zhang, S.C., Wang, Y.J., et al., 2011. Forming condition and enrichment mechanism of the Nanpu Oilfield in the Bohai Bay Basin, China. Acta Geol. Sin. 85 (1), 97–113. https://doi.org/10.19762/j.cnki.dizhixuebao.2011.01.007.

Zoback, M.D., Harjes, H.P., 1997. Injection-induced earthquakes and crustal stress at 9 km depth at the KTB deep drilling site, Germany. J. Geophys. Res. Solid Earth 102 (B8), 18477–18491. https://doi.org/10.1029/96jb02814.